
Proceedings Paper:
Suwansawang, Sopapun and Halliday, David M. (2020) Wavelet-based method for coherence analysis with suppression of low frequency envelope modulation in non-stationary signals. In: 2020 8th International Electrical Engineering Congress, iEECON 2020. 8th International Electrical Engineering Congress, iEECON 2020, 04-06 Mar 2020 2020 8th International Electrical Engineering Congress, iEECON 2020. IEEE, THA.

https://doi.org/10.1109/iEECON48109.2020.229461

Wavelet-based method for coherence analysis with suppression of low frequency envelope modulation in non-stationary signals

Sopapun Suwansawang
Faculty of Science and Technology
Nakhon Pathom Rajabhat University, Thailand
Email:sopapun@webmail.npru.ac.th

David M. Halliday
Department of Electronic Engineering
University of York, UK
Email: david.halliday@york.ac.uk

***Abstract*—Techniques for non-stationary signal analysis are important in understanding dynamical behaviour of complex systems. Time-frequency coherence is widely used to study time-varying properties of non-stationary signals. In this study, we present a wavelet-based method, using Airy wavelet, for coherence analysis. The approach incorporates a novel technique for removal of low frequency components due to envelope modulation in non-stationary signals. The technique is demonstrated on synthetic and real neurophysiological data. Results not only provide a clear description of desired features in non-stationary signals, but also suppress low frequency components due to envelope modulation. Our novel technique shows an effectiveness in extracting features hidden within the signals. It may lead to improved results in coherence analysis of medical, biological, physical and geophysical data containing low frequency envelope modulation besides non-stationarities.**

***Index Terms*—baseline correction, non-stationary analysis, analytic wavelets, signal processing.**

I. Introduction

In nature, most signals exhibit different types of non-stationary and time-varying characteristics. To study time-varying properties of non-stationary signals, analytic wavelets provide a powerful time-frequency analysis framework [1], [2]. The wavelet transform is a localised transform in both time and frequency. This can be achieved by mapping a one-dimensional time-domain signal into a two dimensional representation in time-frequency representation of the signal, and provide time-frequency decomposition of a signal with the possibility to adjust the time-frequency resolution [3].

There are a number of popular measures used to investigate and characterise non-stationary signals. Here, we focus on wavelet coherence analysis which is widely used to detect time-localized common oscillations in bivariate non-stationary signals. It has been applied in many signal processing application, such as biomedical and biological signal processing [1], [4], [5]. However, low frequency components due to envelope modulation may occur in neurophysiological recordings. For example, when recording electromyographic signals (EMG) during walking, low frequency envelope modulation is an important issue [5]–[7]. These have a frequency spectrum that may contaminate the low-frequency part of the EMG frequency spectrum, and may lead to an erroneous interpretation of the signals.

In this paper, a wavelet-based method for coherence analysis with suppression of low frequency envelope modulation in non-stationary signals is presented. The measure is derived from the same two-parameter family of generalized Morse wavelets.

This paper is organised in four sections. Section I introduces the conceptual overview of approach. Section II provides details of signal processing and analysis techniques. Section III shows examples of application to synthetic and real neurophysiological data. Conclusion is included in Section IV.

II. Methods

This section provides details of the proposed technique for wavelet coherence analysis of non-stationary signals that can separate desired signals from effects due to envelope modulation.

A. The generalized Morse wavelets

Generalized Morse wavelets are a two-parameter family of exactly analytic wavelet transform with vanishing support on negative frequency axis [8]. They have been used for studying time-varying properties of non-stationary signals [1], [2]. Time-frequency localisation of generalized Morse wavelets is controlled by β and γ. The parameter β controls the time-domain decay, and γ controls the frequency-domain decay. Also, β and γ can be interpreted as a compactness parameter and a symmetry parameter, respectively [8]. Normally, β and γ are greater than zero. By varying β and γ, the generalized Morse wavelets provide a wide variety of forms. A definition of zeroth-order $(k = 0)$ generalized Morse wavelets in the frequency domain form is provided in [9] as

$$\Psi_{\beta,\gamma}(\omega) = \sqrt{2}H(\omega)A_{k;\beta,\gamma}\omega^{\beta}e^{-\omega^{\gamma}} \tag{1}$$

where $H(\omega)$ is the Heaviside unit step function and $A_{k;\beta,\gamma}$ is a normalising constant that can be expressed by

$$A_{k;\beta,\gamma} = \sqrt{\pi\gamma 2^{r}\Gamma(k + 1/\Gamma(k + r))} \tag{2}$$

978-1-7281-3076-7/20/$31.00

where $\Gamma(\bullet)$ denotes the gamma function and $r = (2\beta+1)/\gamma$. The maximum amplitude occurs at the peak frequency [10],

$$\omega_{\beta,\gamma} \equiv \left(\frac{\beta}{\gamma}\right)^{\frac{1}{\gamma}} \tag{3}$$

The rescaled second derivative of the frequency-domain wavelets evaluated at its peak frequency is $P^2_{\beta,\gamma} \equiv \beta\gamma$, and $P_{\beta,\gamma}$ is called the dimensionless wavelet duration [11], defined as

$$P_{\beta,\gamma} \equiv \sqrt{\beta\gamma} \tag{4}$$

The duration or inverse bandwidth $P_{\beta,\gamma}$ sets the number of oscillations that can fit into the time-domain wavelet's centre window at its peak frequency. It is worth to note that Eq. (3) and (4) are key properties which depend only on two parameters, β and γ. With increasing β at fixed γ, the wavelet becomes more oscillatory in the time domain or more tightly peaked in the frequency domain [11], as seen in Figure 1. Figure 1 is an example of one member of the generalized Morse wavelet family. The $\gamma = 3$, called Airy wavelet, was found to have a high degree of symmetry in the frequency domain. More details regarding the different roles of β and γ in controlling wavelet properties can be found in [8], [10], and [11].

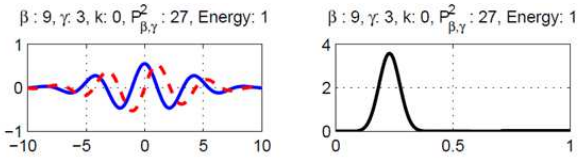

Fig. 1. Example of Airy wavelet for $\beta = 9$, with time domain form $\psi_{\beta,\gamma}(t)$ (left) and frequency domain form $\Psi_{\beta,\gamma}(\omega)$ (right). In the time domain, the plot gives real part (the solid line) and imaginary part (the dashed line) of the wavelet. Frequency f is in cycles per second (Hz). Time is in second (s)

B. Wavelet coherence estimates with suppression of low frequency envelope modulation

Wavelet coherence analysis for removal of low frequency envelope modulation, called practical coherence analysis, is inspired by the study of [12], who compare two coherence estimates. An analysis of time-frequency (τ, f) coherence estimates using wavelets requires estimates for the cross spectrum $(\hat{S}_{xy}(\tau, f))$ and auto spectra $(\hat{S}_x(\tau, f))$, $(\hat{S}_y(\tau, t))$ between two signal, $x(t)$ and $y(t)$, which is given by

$$|\hat{R}_{xy}(\tau, f)|^2 = \frac{|\hat{S}_{xy}(\tau, f)|^2}{\hat{S}_x(\tau, f)\hat{S}_y(\tau, f)} \tag{5}$$

where

$$\hat{S}_x(\tau, f) = \frac{1}{N}\sum_{n=1}^{N} |W_{x;n}(\tau, f)|^2 \tag{6}$$

$$\hat{S}_y(\tau, f) = \frac{1}{N}\sum_{n=1}^{N} |W_{y;n}(\tau, f)|^2 \tag{7}$$

$$\hat{S}_{xy}(\tau, f) = \frac{1}{N}\sum_{n=1}^{N} W_{x;n}(\tau, f)W^*_{y;n}(\tau, f) \tag{8}$$

where $W_{x;n}(\tau, f)$ and $W_{y;n}(\tau, f)$ are the continuous wavelet transforms for signals $x(t)$ and $y(t)$ of trial n, respectively. $*$ indicates conjugate. N is the number of trials.

In our case we compare the original coherence estimate from desired signals with another derived from surrogate data. These surrogate data are calculated from the same signals $x(t)$ and $y(t)$, using Eq. (10), but after shuffling the order of all trials for $y(t)$. Then, Fisher's z-transform, $\tanh^{-1}$, is applied to two coherence estimates.

$$\hat{z} = \tanh^{-1}(|\hat{R}_{xy}(\tau, f)|) \tag{9}$$

where $|\hat{R}_{xy}(\tau, f)|$ is called magnitude coherency, with coherency defined by

$$\hat{R}_{xy}(\tau, f) = \frac{\hat{S}_{xy}(\tau, f)}{\sqrt{\hat{S}_x(\tau, f)\hat{S}_y(\tau, f)}} \tag{10}$$

where $\hat{S}_x$, $\hat{S}_y$, and $\hat{S}_{xy}$ are obtained from Eq. (6), (7), and (8), respectively. Coherency functions are complex valued, and both phase and amplitude coupling contribute to magnitude-squared coherence [12]. We use $\hat{D}_C$ to represent the practical coherence analysis. $\hat{D}_C$ is calculated as

$$\hat{D}_C = \tanh\{\hat{z}_C - \hat{z}_{CS}\} \tag{11}$$

where $\hat{z}_C$ and $\hat{z}_{CS}$ are Fisher's z-transform of coherence estimates from original data and surrogate data, respectively.

A priori hypothesis on the relationship between two signals is required. i) if two z transformed coherence estimates, $\hat{z}_C$ and $\hat{z}_{CS}$, have similar values, $\hat{D}_C$ will tend to be small. ii) if $\hat{z}_C$ is affected by low frequency envelope modulation component and $\hat{z}_{CS}$ is expected to indicate where the low frequency envelope modulation component is consistent across segment, $\hat{D}_C$ should have significant values outside that low frequency envelope modulation. iii) Value of $\hat{D}_C$ depends on $\hat{z}_C$ if $\hat{z}_C$ is unrelated to $\hat{z}_{CS}$.

It is necessary to decide which of the coherence values are significant. A confidence interval is used to determine if the wavelet coherence is significantly different from zero. If the two signals are independent and have Gaussian distributions, the distribution of the coherence estimate is given as $Pr(R^2 \leq r) = 1 - (1-r)^{K-1}, 0 \leq r \leq 1$. If the confidence interval value of 95% is chosen, then the detection threshold value is $r_{95\%} = 1 - 0.05^{1/(K-1)}$ [4].

III. Application

For testing and validation, practical coherence analysis is explored further by analysing surrogate and real data. Here, the proposed technique is expected to clarify the hypothesis stated in Section II-B.

In this section, the simulated signals are generated using the generative model of oscillatory synchronisation proposed by [13], which is similar to the well-known Kuramoto model

[14]. The discrete phase-evolution of oscillators X and Y used in this study can be defined by

$$\phi_x(t+1) = \phi_x(t) + h\left(\omega_x(t) + N_p^x(t)\right) \tag{12}$$

$$\phi_y(t+1) = \phi_x(t) + h\left(\omega_y(t) + \kappa \sin(\phi_y(t) - \phi_x(t)) + N_p^y(t)\right) \tag{13}$$

where ϕ_x and ϕ_y are the phase evolution of oscillator X and Y, respectively, $N_p(t)$ is an intrinsic phase noise process, $\omega(t)$ is an intrinsic frequency, and κ is the coupling strength.

The simulated signals have a centre frequency of 8 Hz, an intrinsic frequency differences between oscillator X and Y called detuning frequency (Δf) of 3 Hz, and coupling strength of 0.5. Step size h is set to 1 ms. Intrinsic noise is 0.05 and SNR is 250. Three envelope windows, including 1-Hz and 5-Hz triangular waves, and 3-Hz half wave rectified sine waves, are then applied to simulated signals. Here, a key aspect of our envelope windows is a substitution model of low frequency envelope modulation that allows its exact behaviour to be predicted, for example, frequency and amplitude. So, 100 datasets of the simulated signals modulated with envelope windows are called the test signals shown in Figure 2(A)(column 1-3).

To further understand the nature of the practical coherence analysis for removal of low frequency envelope modulation, we consider a practical example of using the proposed technique. An example of its application to real sEMG data is demonstrated. Here, rectified sEMG signals, Figure 2(A)(column 4) obtained from one subject treadmill walking taken from a previous study of [6], are used to validate the reliability of the proposed technique.

Wavelet coherence and practical coherence analysis are used in displaying features of the signals and the performance of the technique calculated using averages over 100 trials. All measures have a segment length of 1000 ms for the test signals, and 1024 ms non overlapping epochs from one subject during treadmill walking for real EMG signals. They are computed using Airy wavelet with $\beta = 9$. The significant value for wavelet coherence is considered if the estimate is greater than the 95% confidence interval. In this study, The 95% confidence interval for practical coherence estimates is 0.029 based on analysis of 100 trials. The results are shown in Figure 2(B-D).

Fisher's z-transform of coherence estimates from three test signals ($\hat{z}_C$) illustrated in Figure 2(B)(column 1-3) show that strong peak magnitude of oscillatory synchronisation occurs at frequencies 5-10 Hz around 200-500 ms (Figure 2(B)(column 1)), at 5-15 Hz around 300-600 ms (Figure 2(B)(column 2)), and at 5-6 Hz around 200-400 ms and 800-1000 ms (Figure 2(B)(column 3). Figure 2(B)(column 4) shows that the EMG-EMG coherence consist of a significant low-frequency component (<5 Hz) present throughout the step cycle together with weaker peaks of coherence arising between 8 and 12-30 Hz around early and late swing of step cycle.

Figure 2(C) shows Fisher's z-transform of coherence estimates from surrogate data ($\hat{z}_{CS}$). The results in Figure 2(C)(column 1 and 2) indicate that there is no coherence between the data. In Figure 2(C)(column 3), the result shows peak at low frequency of 5 Hz in the beginning and the end of the time window. Importantly, the significant features in terms of centre frequency of 8 Hz $\pm$ 3 Hz at time 200-600 ms shown in Figure 2(B)(column 1-3) disappear in Figure 2(C)(column 1-3). Also, weaker peaks of EMG-EMG coherence between 8 and 12-30 Hz around early and late swing of step cycle in Figure 2(B)(column 4) disappear as seen in Figure 2(C)(column 4). Thus, the practical coherence estimates ($\hat{D}_C$) in Figure 2(D) indicate that low frequency components due to envelope modulation disappear, and a distinct 8 Hz $\pm$ 3 Hz correlation located around 200-600 ms remains, as clearly seen in Figure Interestingly, low frequency (<5 Hz) components seen in Figure 2(D)(column 1-3). More importantly, it is clearly seen that distinct frequencies 8 Hz and 12-30 Hz located around early and late swing, but the low frequency components (< 5 Hz) disappear as illustrated in Figure 2(D)(column 4). [6] reported that coherence between 12 and 32 Hz is commonly seen and has been demonstrated to represent a rhythmic modulation of motor unit activity. The proposed technique gives advantage in terms of extracting low frequency components due to envelope modulation, and detecting the correlations where the coherence has significant features.

IV. Conclusion

We propose a novel technique for removal of low frequency envelope modulation in coherence analysis using generalized Morse wavelets. The technique compares the original coherence from the test signals with another derived from surrogate data shown in Section II. We demonstrate the technique with synthetic data. Three examples are presented in section III.

The results from practical coherence estimates are consistent in terms of centre frequency of 8 Hz $\pm\Delta f$ 3 Hz around time range 200-600 ms as a designated by the generative model. When the new technique does suppress the envelope modulation it is most likely to reduce low frequencies due to envelope windows, 1-Hz and 5-Hz triangular waves, and 3-Hz half wave rectified sine waves, as clearly seen in Figure 2(D), especially Figure 2(D)(column 3). The results from real EMG signals analysis show that the low frequency components (< 5 Hz) are removed while a rhythmic modulation of motor unit activity (8 and 12-30 Hz) around early and late swing remains unchanged, as clearly seen in Figure 2(D)(column 4).

Our results calculated by Eq. (11) suggest that the method is able to successfully detect localised correlation in the time frequency plane. The technique in this study can serve as a useful tool for investigating and characterising the interaction between non-stationary signals. It can be used to separate physiological mechanisms from effects due to envelope modulation. There may still be valid effects due to low frequency envelope modulation, now we hope to get a clearer and more accurate assessment of these.

References

[1] J.-S. Brittain, D. Halliday, B. Conway, and J. Nielsen, "Single-trial multiwavelet coherence in application to neurophysiological time series,"

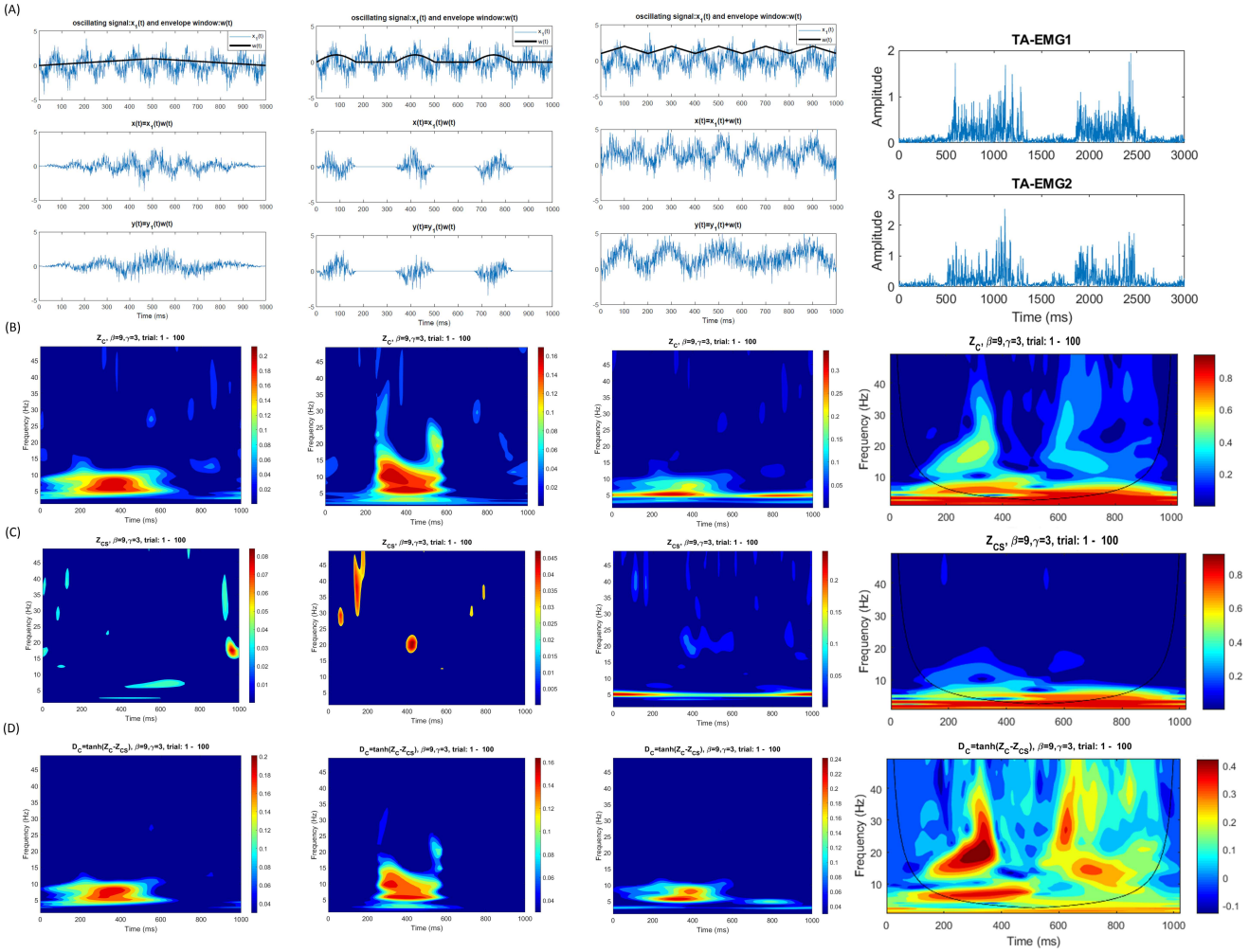

Fig. 2. The signals and time-frequency analysis from Airy wavelet (γ = 3 and β=9) for 100 trials of signals. One trial of test signals generated using generative model of oscillatory synchronisation given by Eq. (12) and (13) modulated with envelope windows are shown in (A) column 1-3, and two steps of real EMG signals are shown in (A) column 4. Fisher's z-transform of coherence estimates from the test signals and the surrogate data are shown in (B) and (C), respectively. Practical coherence estimates are shown in (D)

IEEE Transactionson Biomedical Engineering, vol. 54, no. 5, pp. 854–862, 2007.

[2] A. Nakhnikian, S. Ito, L. Dwiel, L. Grasse, G. Rebec, L. Lauridsen, and J. Beggs, "A novel cross-frequency coupling detection method using the generalized morse wavelets," *J. Neurosci. Methods*, vol. 269, pp. 61–73, 2016.

[3] P. Addison, *The illustrated wavelet transform handbook*. IOP Publishing Ltd, 2002.

[4] Y. Zhan, D. Halliday, P. Jiang, X. Liu, and J. Feng, "Detecting time-dependent coherence between non-stationary electrophysiological signal-a combined statistical and time-frequency approach," *J. Neurosci. Methods*, vol. 156, pp. 322–332, 2006.

[5] S. Suwansawang and D. Halliday, "Time-frequency based coherence and phase locking value analysis of human locomotion data using generalized morse wavelets," in *Proceedings of the 10th International Joint Conference on Biomedical Engineering Systems and Technologies (BIOSTEC 2017) - Volume 4: BIOSIGNALS*, Porto, Portugal, Feburary 2017, pp. 34–40.

[6] D. Halliday, B. Conway, Christensen, N. Hansen, N. Petersen, and Nielsen, "Functional coupling of motor units is modulated during walking in human subjects," *J Neurophysiol*, vol. 89, pp. 960–968, 2003.

[7] J.-S. Brittain, "The non-stationary analysis and characterisation of neurological systems involved in human locomotion," Ph.D. dissertation, Univ. of York, York, 2007.

[8] J. Lilly and S. Olhede, "High-order properties of analytic wavelets," *IEEE Transactions on signal processing.*, vol. 57, no. 1, pp. 146–160, 2009.

[9] S. Olhede and A. Walden, "Polarization phase relationships via multiple morse wavelet. i fundamentals," *Proc. Roy. Soc. Lond*, vol. 60, no. 11, pp. 6036–6041, 2003.

[10] J. Lilly and S. Olhede, "Generalized morse wavelet as a superfamily of analytic wavelets," *IEEE Transactions on Signal Processing*, vol. 60, no. 11, pp. 6036–6041, 2012.

[11] ——, "On the analytic wavelet transform," *IEEE Transactions on Information Theory*, vol. 56, pp. 4135–4156, 2010.

[12] A. Amjad, D. Halliday, J. Rosenberg, and B. Conway, "An extended difference of coherence test for comparing and combining several independent coherence estimates: theory and application to the study of motor units and physiological tremor," *Journal of Neuroscience Methods*, vol. 73, pp. 69–79, 1997.

[13] E. Lowet, M. Roberts, P. Bonizzi, J. Karel, and P. Weerd, "Quantifying neural oscillatory synchronization: A comparison between spectral coherence and phase-locking value approaches," *PLoS one*, vol. 11, no. 1, pp. 1–37, 2016.

[14] M. Breakspear, S. Heitmann, and A. Daffertshofer, "Generative models of cortical oscillations: neurobiological implications of the kuramoto model," *Frontiers in Human Neuroscience*, vol. 4, p. 190, 2010.